



Association of type I neurons positive for NADPH-diaphorase with blood vessels in the adult monkey corpus callosum

Kathleen S. Rockland^{1,2*} and Naema Nayyar²

¹ Laboratory for Cortical Organization and Systematics, RIKEN Brain Science Institute, Wako-shi, Saitama, Japan

² Picower Institute of Learning and Memory, Massachusetts Institute of Technology, Cambridge, MA, USA

Edited by:

Yoshiyuki Kubota, National Institute for Physiological Sciences, Japan

Reviewed by:

Noritaka Ichinohe, National Center of Neurology and Psychiatry, Japan
Bruno Cauli, CNRS and UPMC, France

*Correspondence:

Kathleen S. Rockland, RIKEN-MIT Center for Neural Circuit Genetics, Picower Institute for Learning and Memory, Massachusetts Institute of Technology, 77 Massachusetts Avenue, Building 46, Cambridge, MA 02139, USA.
e-mail: kathrock@mit.edu

Sagittal sections through the corpus callosum of adult macaque monkeys ($n = 7$) reveal a subpopulation of neurons positive for NADPH-diaphorase (NADPHd). These are sparsely distributed, with 2–12 neurons scored over the anterior two-thirds of the callosum (about 14 mm). Neurons are densely labeled, type 1; but on the basis of soma and dendritic morphology, these neurons exhibit distinct heterogeneity. In one subpopulation, the cell body is narrowly attenuated (7–10 μm in width). These have bipolar dendrites, extending 300–800 μm from the cell body. One or both of the dendrites is often closely associated with blood vessels and tends to be aligned dorso-ventral, perpendicular to the body of the callosum. Another subpopulation of neurons has a larger soma (typically, 15 $\mu\text{m} \times 20 \mu\text{m}$) and more multipolar dendrites, which are not as obviously associated with blood vessels. White matter neurons positive for NADPHd have previously been observed as a transient population, most numerous during development, in the human corpus callosum, as well as in that of other species. Their persistence in the corpus callosum of adult macaques and their close association with blood vessels has not previously been reported and is suggestive of roles other than axon guidance.

Keywords: neurovascular, white matter neurons, acetylcholine, callosal septa

INTRODUCTION

GABAergic neurons in the cortical white matter (WM) have been repeatedly demonstrated in multiple species (Kostovic and Rakic, 1980; Sandell, 1986; Chun and Shatz, 1989; Yan et al., 1996; Clancy et al., 2001; Jovanov-Milosevic et al., 2009; Suarez-Sola et al., 2009). Recent experiments have shown that at least some of these send long-distance connections into the cortical gray matter (Tomioka et al., 2005; Tomioka and Rockland, 2007; Higo et al., 2009), and thus presumably have a significant role in the cortical circuitry.

White matter neurons occur either subjacent to layer 6 or deeper in the WM core (Clancy et al., 2001; García-Marín et al., 2010). A subset has been identified within the parenchyma of the corpus callosum, where a role in circuitry might seem less likely. Since these neurons are more abundant in development, they have been considered as likely to figure in processes of axon guidance (Riederer et al., 2004; Niquille et al., 2009).

In this paper, we demonstrate that neurons positive for NADPH-diaphorase (NADPHd+) occur in the corpus callosum of adult macaque monkeys. NADPH-diaphorase is an enzyme that oxidizes the reduced form of nicotinamide adenine dinucleotide phosphate (NADPH), and is found in a small population of GABAergic neurons (reviewed in Yan et al., 1996). The population of NADPHd+ neurons has been further subdivided into at least two broad categories: type 1, with a larger soma (diameter > 20 μm ; Yan et al., 1996) and dense, Golgi-like staining and type 2, with smaller soma and lighter more diffuse staining. The neurons reported here uniformly belong to the densely stained

type 1 subpopulation, but exhibit distinct variability of soma size and dendritic arbors. Some of these neurons are conspicuously associated with blood vessels. This localization in the corpus callosum and the persistence into adulthood are strongly suggestive of roles other than in axon guidance.

MATERIALS AND METHODS

Tissue from seven adult macaque monkeys (4–6 kg) was used in this study. Monkeys were sedated with ketamine (11 mg/kg i.m.), deeply anesthetized with an overdose of Nembutal (75 mg/kg), and perfused transcardially in sequence with 0.9% saline, 4% paraformaldehyde, and three runs (250, 250, and 500 ml) of chilled 0.1 M phosphate buffer (PB) with 10, 20, or 30% sucrose, respectively. Brains were removed from the skull, bisected in the midline, placed in cold 30% sucrose until sinking (1–2 days), and cut serially in the sagittal plane (at 50 μm) by frozen microtomy. Three of the hemispheres had unilateral injections of biotinylated dextran amine in a sterile surgery procedure, 18–21 days before the perfusion (Zhong and Rockland, 2003). All animal procedures were carried out in conformity with institutionally approved protocols (RIKEN, Brain Science Institute), and in accordance with the US National Institutes of Health Guide for the Care and Use of Laboratory Animals.

For six of the seven hemispheres, alternate sections were reacted for NADPHd (Scherer-Singler et al., 1983). Substrate solution contained, per 50 ml of Tris buffer (TB; pH 7.4), 400 μl Triton-X, 40 mg NADPH (Sigma-Aldrich), 35 mg Nitroblue tetrazolium

(Sigma-Aldrich), and 60 mg sodium malate (Fisher Scientific). Tissue sections were rinsed in TB and incubated free-floating, in 8-compartment, netted “pie-plate” holders, at 37° until the desired intensity of staining was reached (usually about 45–90 min). Degree of staining was evaluated by viewing wet tissue under a dissecting microscope. At completion of the reaction, tissue was rinsed 3× in TB, mounted onto coated slides, dehydrated, and coverslipped. A second series of alternating sections was reacted by immunocytochemistry for parvalbumin (PV) or acetylcholinesterase (AChE). One hemisphere (R116) was processed in repeating series of three for NADPHd, acetylcholinesterase, and calbindin (the latter is not reported). The additional procedures were initially carried out as part of other studies. We include here results from the PV and AChE processing, since (1) there is an established link between AChE positive fibers and NADPHd+ neurons (Vaucher et al., 1997; Kalinchuk et al., 2010; Kilduff et al., 2011) and (2) continued work on the distribution of NADPHd+ neurons may show a relationship to what appear to be PV+ compartments.

PV immunohistochemistry was carried out on free-floating sections. These were placed for 1 h at room temperature, in 0.1 M phosphate buffered saline (PBS; pH 7.3), containing 0.5% Triton-X 100 and 5% normal goat serum (PBS-TG), and then incubated for 40–48 h at 4°C with PBS-TG containing mouse monoclonal anti-PV antibody (Swant, Bellinzona, Switzerland; 1:50,000). After rinsing, sections were continued to biotinylated goat anti-mouse IgG (Vector Laboratories, Burlingame, CA, USA; 1:200) for 1.5 h at room temperature. Immunoreactivity was visualized by the ABC protocol (one drop of reagent per 7 ml of 0.1 M PB; ABC Elite kits; Vector), followed by diaminobenzidine histochemistry with 0.03% nickel ammonium sulfate. Sections were mounted, dehydrated, and coverslipped. AChE histochemistry was carried out on free-floating sections, according to a standard protocol (Geneser-Jensen and Blackstad, 1971). Incubation time in substrate was prolonged to 2–3 days at room temperature, for the sake of enhancing reaction product in the comparatively AChE-poor cortical regions.

DATA ANALYSIS

Analysis was restricted to the medial most portion (1–2 mm) of the corpus callosum, in order to avoid confounds with the adjoining, non-callosal WM. Midline was determined by reference to the midline of the gross brain, as bisected after removal from the skull, and by reference to adjoining structures. That is, sections of interest were medial to the caudate nucleus. The posterior most portion of the corpus callosum (splenium) was not available. For the seven brains, the available portion of the corpus callosum comprised the anterior most 6, 7, 10, 15, 15, 22, and 25 mm.

Sections were scanned by using an Olympus VS120 light microscope equipped with a VC50 camera, captured by using a 10× or 40× objective (equivalent to 100× or 400× base magnification), and digitized as virtual slides. Most of the higher magnification scans were acquired in Z-mode to utilize the extended depth of focus feature. Sections were scored for number of cells positive for NADPHd; and these cells were subsequently analyzed for soma size and dendritic features. Long and short axes of the soma were obtained using VS120 measurement tools applied to the metadata

of the captured image. Size, brightness, and contrast were adjusted to reflect the real image, by Photoshop software (Adobe Systems, San Jose, CA, USA).

RESULTS

In all seven brains, neurons positive for NADPHd occurred in the parenchyma of the corpus callosum. These were sparsely distributed, with 2–12 neurons per section (**Figure 1**). Neurons were typically isolated, but groups of three to four neurons, spaced 500–700 μm apart, were also found, especially in the region of the genu (**Figure 2**).

In addition to the sparsely scattered NADPHd neurons within the corpus callosum, positive neurons were evident along both the dorsal and ventral margins. These were less sparsely distributed (**Figures 1 and 3**); but since we consider these as a separate sub-population, on the grounds of location and orientation, they were not included in further analysis. NADPHd neurons with soma within 100 μm of either margin were also excluded.

Positive neurons were densely filled, in Golgi-like detail, and therefore unambiguously classified as type 1 (Yan et al., 1996; Estrada and DeFelipe, 1998). No examples of type 2 neurons, defined as small, lightly stained neurons, were evident. Within the broad category of type 1, however, further sub-populations were indicated on the basis of several morphological criteria. First, soma size and shape were distinctly varied (**Figures 1–4**). Soma size ranged from 12.5 to 44.3 μm in the long axis and 4.5–13.6 μm in the short axis (**Table 1**). A few neurons had somas that were almost round; but the majority had an elongated soma, where the long axis was two or three times the length of the short axis (four times, for cell 11, R30). For four brains, the average length and width was calculated: R30, 20.4 μm × 8.3 μm; R31, 22.7 μm × 10.8 μm; P3, 26.1 μm × 11.4 μm; R19L, 19.9 μm × 10.7 μm (see **Table 1**).

Second, the configuration of proximal dendrites was distinctive. Two broad groupings on the basis of primary branch configuration at the soma are: bipolar or multipolar (**Figures 1–4**). Within the multipolar group, a small further subset could be identified by having one notably thick side dendrite (**Figure 3D**).

Third, the dendritic arborization could be described as bipolar, bitufted, multipolar, or asymmetric, with one vertical and one multipolar dendrite (**Figures 2–4**). Dendrites could commonly be followed 350–550 μm from the soma in single sections. These were typically beaded, but could also have a sparse distribution of spines (**Figures 1 and 4**). A striking feature was the close association of the bipolar neurons in particular with blood vessels (**Figures 3E and 4C–E**). Dendrites of multipolar neurons often approached blood vessels (**Figures 2 and 4**), but it was hard to judge if these actually formed direct contacts.

Morphological heterogeneity has been previously reported for NADPHd+ neurons in the cortical gray matter (Estrada and DeFelipe, 1998). In our sample, strictly bipolar neurons (**Figures 3E and 4E**), with two oppositely oriented primary dendrites extending distally, were a small minority. Either the ascending or descending dendrite was often tightly intertwined with one or more branches. Bitufted cells were more frequently observed (**Figure 4C**); and multipolar neurons were the most numerous (**Figures 3C and 4A**). As our material consisted of alternating, not sequential, sections,

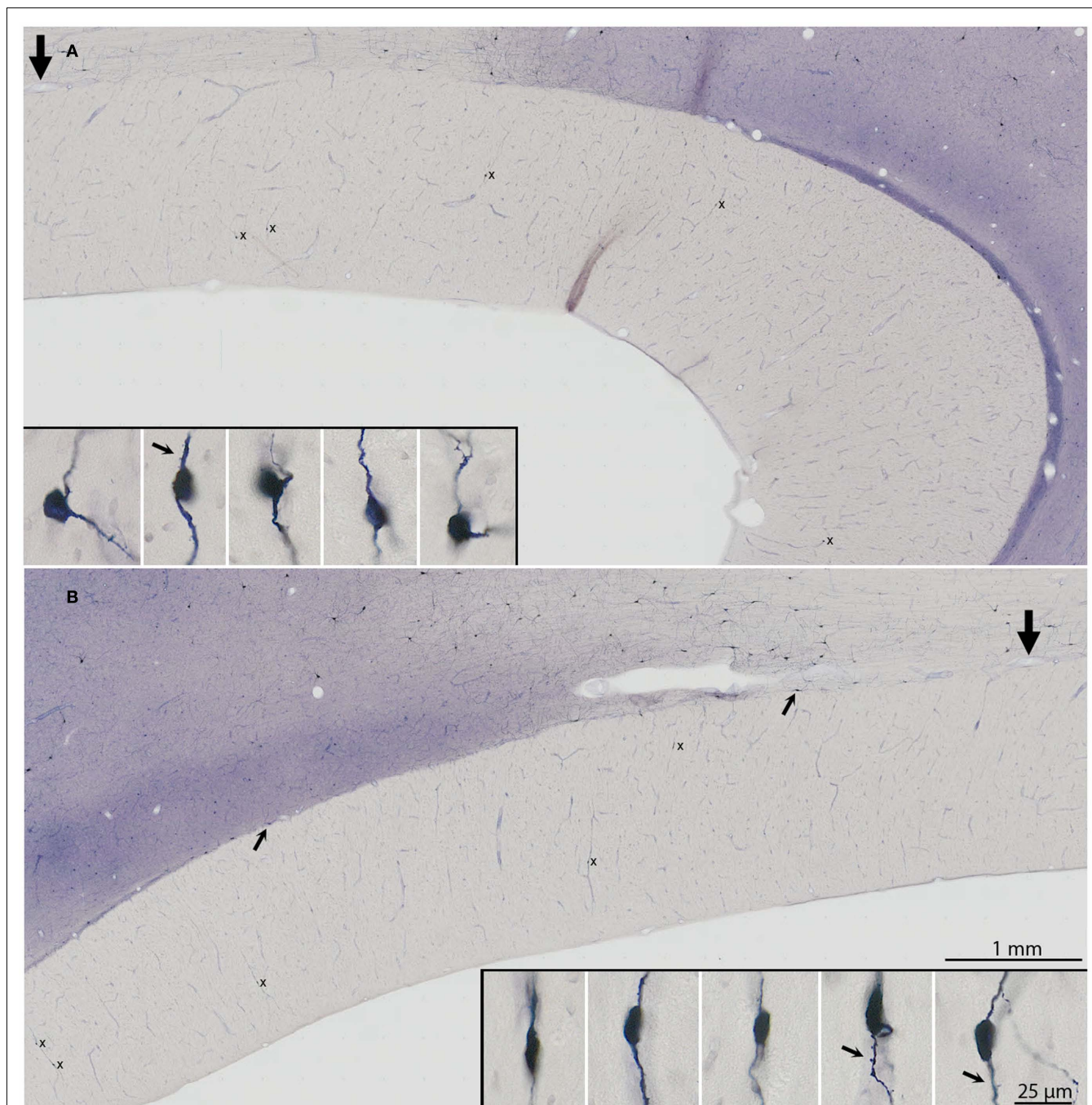


FIGURE 1 | (A,B) Low magnification photomicrograph of a mid-sagittal section through the corpus callosum in case R30. **(B)** is a posterior continuation of the portion in **(A)**, such that the thick arrows in **(A,B)** demarcate corresponding blood vessels. Ten neurons that are NADPHd+ are identified, and indicated by x in **(A,B)**. Somas and proximal dendrites of these neurons are shown in higher magnification insets. The five neurons in **(A)** are

arranged from anterior (at right) to posterior (at left), and the lower five, similarly, for the segment shown in **(B)**. Arrows in three of the insets point to sparsely distributed dendritic spines. Neurons have been rotated so that the major axis is perpendicular to the dorsal surface of the brain. NADPHd+ neurons are also obvious at the dorsal margin of the callosum [two small arrows in **(B)**] and in the overlying cortical white matter.

we are limiting ourselves to these observations, which will need to be followed up by more detailed analysis and/or additional criteria for classifications.

Finer processes, possibly corresponding to axons, could often be identified (**Figure 3D**, inset), but no close association with blood vessels could be confidently discerned.

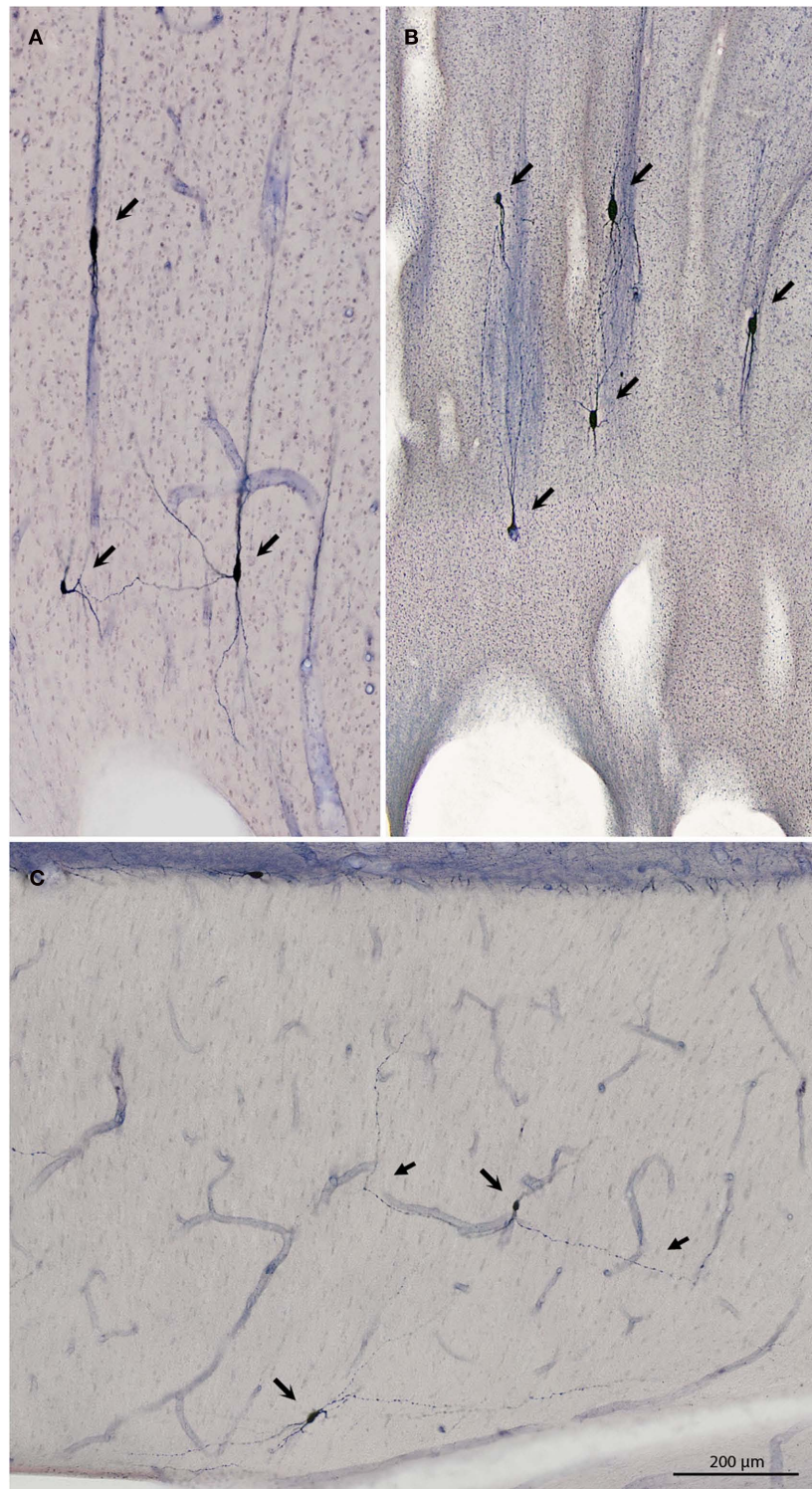


FIGURE 2 | Three examples of small groups of NADPHd+ neurons. (A) Three neurons (arrows), at the genu (case R30). The dendritic portion of a fourth neuron is visible at the right. **(B)** Five neurons (arrows), also at the genu (case P3). In **(A,B)**, the field has been rotated 90° counter-clockwise, for the

sake of formatting. **(C)** Two neurons (right pointing arrows) in the body of the callosum (case R31). Distal portions of the dendrite of the more dorsal neuron are indicated by left-pointing arrows. The left dendrite parallels one of the blood vessels for >200 μm.

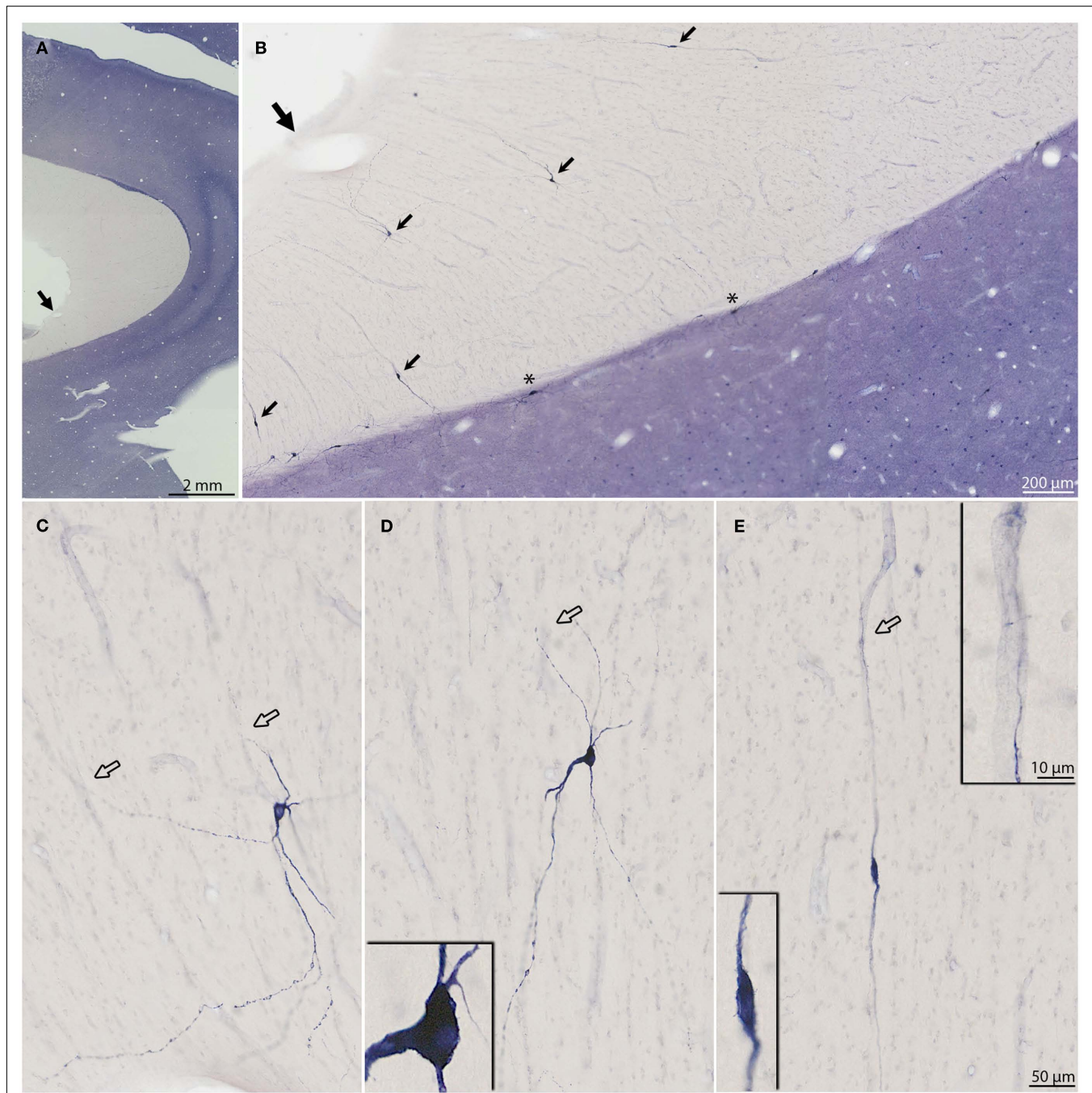


FIGURE 3 | (A,B) Progressively higher magnifications of a mid-sagittal section through the corpus callosum in R31. Thick arrows demarcate corresponding blood vessels in (A,B). Scattered neurons that are NADPHd+ are evident at the ventral margin of the callosum [asterisk in (B)]. Five neurons positive for NADPHd are indicated by short arrows in (B). (C–E) Higher magnification views of three of the NADPHd+ neurons to show dendritic detail. Inset in (D) is an example of a neuron

with one very thick dendrite. Inset in [(E) at lower left] is an example of a neuron with thin soma and bipolar dendritic arborization. Inset in [(E) at upper right] shows close association of dendrite and blood vessel. Individual neurons have been rotated so that they are approximately perpendicular to the dorsal surface of the brain. Hollow arrows indicate points where NADPHd+ dendrites are in close proximity to blood vessels.

OTHER MARKERS

In one brain, stained for acetylcholinesterase (AChE), occasional neurons were evident in the callosum (Figure 5). AChE+ fibers were also detected. These were usually

oriented dorso-ventrally, perpendicular to the long axis of the corpus callosum (Figure 5). Positive neurons were not found in tissue stained for parvalbumin (PV; Figure 6).

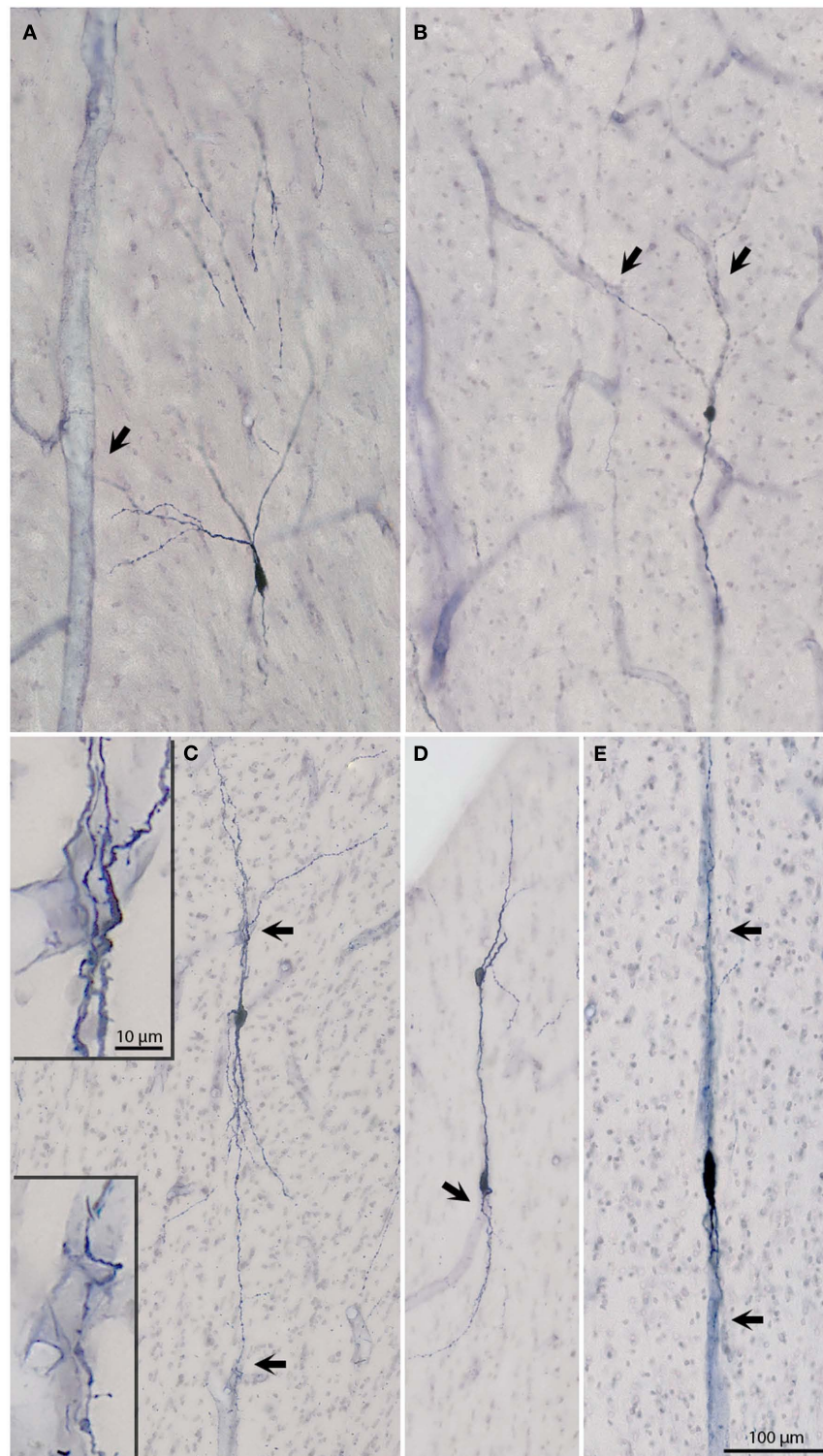


FIGURE 4 | (A–E) Micrographs of six additional NADPHd+ neurons to show soma and dendritic arbors. Arrows point to blood vessels, which are in apparent close association with dendrites. The association is particularly evident for the neurons in (C–E). The two higher magnification insets in (C) depict dendrites intertwining around blood vessels. Sparse dendritic

spines are evident on both segments. The two vertically aligned neurons in (D), have partially overlapping dendrites, giving an illusory appearance of being conjoined. The neurons in (D) are from the posterior most x in **Figure 1**; the other four neurons are from R19L (A), R31 (B), and R30 (C,E).

Table 1 | Soma size of NADPHd+ intracallosal cells from four brains.

Case	Cell	Length × width (μm)
R30	1 (s. 8A)	15.1 × 9.9
	2 (s. 8A)	15.1 × 8.4
	3 (s. 8A)	13.6 × 9.2
	4 (s. 8A)	12.5 × 7.7
	5 (s. 8A)	18.6 × 4.5
	6 (s. 8A)	15.5 × 6.1
	7 (s. 8A)	18.8 × 8.4
	8 (s. 8A)	21.8 × 6.1
	9 (s. 8B)	16.8 × 8.3
	10 (s. 8B)	16.9 × 10.2
	11 (s. 4B)	29.3 × 6.8
	12 (s. 2C)	29.5 × 11.4
	13 (s. 2C)	19.5 × 7.1
	14 (s. 2C)	44.3 × 11.7
	15 (s. 2C)	19.1 × 8.3
		Average 20.4 × 8.3
R31	1 (s. 4)	22.6 × 12.9
	2 (s. 7)	20.0 × 9.7
	3 (s. 7)	28.4 × 11.5
	4 (s. 7)	32.2 × 10.3
	5 (s. 7)	16.6 × 11.0
	6 (s. 7)	16.1 × 9.1
		Average 22.7 × 10.8
P3	1 (s. 7)	30.5 × 12.5
	2 (s. 7)	20.8 × 8.9
	3 (s. 7)	27.6 × 12.8
	4 (s. 7)	26.2 × 9.1
	5 (s. 7)	23.0 × 10.9
	6 (s. 7)	33.2 × 11.4
	7 (s. 7)	23.2 × 12.7
	8 (s. 7)	25.1 × 12.5
	9 (s. 7)	15.9 × 11.2
	10 (s. 5)	24.0 × 11.5
	11 (s. 5)	31.1 × 12.4
	12 (s. 3)	21.2 × 12.5
	13 (s. 3)	37.3 × 9.8
		Average 26.1 × 11.4
R19L	1 (s. 9)	20.9 × 7.6
	2 (s. 9)	20.9 × 13.4
	3 (s. 9)	19.3 × 12.3
	4 (s. 9)	18.8 × 11.6
	5 (s. 12)	19.9 × 7.7
	6 (s. 12)	19.1 × 11.6
	7 (s. 12)	17.7 × 11.5
	8 (s. 12)	23.8 × 13.6
	9 (s. 12)	16.4 × 9.7
	10 (s. 12)	18.5 × 7.1
	11 (s. 11)	15.8 × 12.0
	12 (s. 11)	27.5 × 10.7
		Average 19.9 × 10.7

Average length × width is given for the four groups of cells. s., Section containing the particular neurons.

CALLOSAL SEPTA

In tissue reacted for PV, alternating zones could be discerned, about 150–200 μm across, where callosal fibers were differentially oriented. That is, PV+ segments were either mainly in cross section (asterisks, **Figure 6**) or occurred in short, obliquely cut segments (arrows, **Figure 6**). The PV+ fibers presumably originate from subpopulations of large, PV+ pyramids in layer 5 of some cortical areas (Ichinohe et al., 2004).

DISCUSSION

One main point of the present report is the persistence of NADPHd+ neurons in the corpus callosum of adult macaque monkeys. Previous reports have demonstrated neurons in the corpus callosum, but have found that these neurons decrease significantly in the postnatal period. In cats, the number drops from about 570 at birth to 200 in the adult, and the distribution becomes restricted to the rostrum (Riederer et al., 2004). In humans, what were called “intracallosal” neurons are most numerous in the second half of gestation and the early postnatal years, but are found only sporadically in the adult brain (Jovanov-Milošević et al., 2010). In our adult monkey material, NADPHd+ neurons were sparsely distributed, but readily identified. Consistent with Riederer et al. although the neurons were found throughout the body of the callosum, the rostrum, and genu was a preferential location (splenium was not examined). Since the present report was restricted to adult material, we cannot comment on a developmentally related decrease in density, although this would seem likely.

A second point is the striking morphological heterogeneity of the NADPHd+ neurons. This feature has consistently been noted in reports dealing with both gray matter and WM populations. Dendritic morphology is described as bipolar, bitufted, or multipolar; and neurons visualized by immuno-staining for nitric oxide synthetase (NOS) are further distinguishable based on whether NOS is co-localized with neuropeptide-Y or somatostatin (Yan et al., 1996; Estrada and DeFelipe, 1998; Cauli et al., 2004).

A third point is the conspicuous association of at least some of these neurons with blood vessels. An association of NADPHd+ neurons with blood vessels has been remarked previously, but primarily as pertains to neurons in the gray matter (Vaucher et al., 1997; Hamel, 2006; Suarez-Sola et al., 2009; Cauli and Hamel, 2010, among others). In the gray matter, NOS+ neurons are considered to act in conjunction with acetylcholine, serotonin, and an assortment of signaling molecules to transmute neural signals to vascular responses, in an activity-related cycle of vasodilatations and constrictions (Cauli et al., 2004; Iadecola, 2004; Kocharyan et al., 2008; Lecrux and Hamel, 2011). Owing to the diffusion properties of NO, a given NOS+ neuron has been estimated to have an effective sphere of influence of about 100 μm radius (Wood and Garthwaite, 1994; Estrada and DeFelipe, 1998), and is thought to influence several microvessels (Cauli et al., 2004). Some of the intracallosal neurons reported here appeared to contact several microvessels. Others, however, seemed closely associated with a single blood vessel (**Figures 3** and **4**). Moreover, in view of the sparse distribution of the NADPHd+ neurons, it is evident that these are associated with only a subset of microvessels.



FIGURE 5 | (A) Low magnification view of a mid-sagittal section through the genu and rostrum of the corpus callosum, reacted for acetylcholinesterase (AChE). **(B,C)** Higher magnifications from upper arrow **(B)** and lower arrow **(C)**, showing AChE fibers and scattered AChE+

neurons (small arrows). The field in **(B)** has been rotated so as to be perpendicular to the dorsal surface of the brain. One neuron [in **(C)**] with thin soma and bipolar proximal dendrites is shown at higher magnification in the box at the right.



FIGURE 6 | (A,B) Two fields through the body of the callosum, reacted for parvalbumin (PV). The location of the two fields is indicated by asterisks in the low magnification inset in **(A)** [(A) is more anterior; (B) is more posterior].

Subpopulations of PV+ fibers are cut predominantly in cross section (asterisks) or oblique section (arrows), with some indication of a regular alternation.

An obvious question is whether the NADPHd+ neurons in the deep WM of the callosum have the same role (i.e., part of an activity-related neurovascular unit) as has been defined for those in the overwhelmingly more cell-dense gray matter. Possibly relevant in this regard is evidence from *in vitro* experiments on rat optic nerve, showing that there are persistent signals from eNOS+ microvascular cells to axons, and that these generate both tonic and phasic nitric oxide (NO) signals (Garthwaite et al., 2006). These results pertain specifically to eNOS, but can be taken to indicate some effect of NO directly on axons. Alternatively, nNOS may figure in activity-dependent modulation of the myelin sheath by an axon (Stys, 2011) or, more particularly, in a neurovascular unit where axons and myelination, not spiking neurons, are the interacting components.

Other recent studies have reported release of vesicular glutamate at discrete sites along axons in the WM (Kukley et al., 2007). This has been interpreted in the context of inotropic glutamatergic receptors on oligodendrocyte precursor cells (Kukley et al., 2007). Given that NO can amplify glutamate release and interact with NMDA receptors (Kara and Friedlander, 1998), this might be another influence of the NADPHd+ neurons.

With the discovery that some NADPHd+ neurons have long-distance projections (Tomioka et al., 2005; Tomioka and Rockland, 2007; Higo et al., 2009), these have also been discussed in a network context; and *in vitro* experiments have verified that WM neurons participate in functional circuitry in the gray matter (Clancy et al., 2001; von Engelhardt et al., 2011). Thus, another possibility is that NADPHd+ neurons in the callosum may participate in a widespread network, either involving neurons in the overlying gray matter or, perhaps more likely given their distance from the gray matter, similar neurons, or neuron–glia–vascular units in the deep WM.

Expression studies of cFOS-labeled neurons have implicated cortical nNOS+ interneurons in slow wave sleep (Kilduff et al.,

2011), although these were described in the cortical gray matter. Another aspect of the sleep cycle, however, is cholinergic input from the basal forebrain (Vaucher et al., 1997; Kalinchuk et al., 2010; Kilduff et al., 2011). Interestingly, we observed cholinergic fibers and cells in the callosum in the present report; but further work will be necessary to determine if there is significant cholinergic input to the intracallosal NADPHd+ cells.

Finally, it is worth noting that NADPHd+ intracallosal neurons tend to have a vertical orientation, extended in the dorso-ventral plane. This may be related to the dorso-ventrally oriented septa described in the developing human callosum (Jovanov-Milošević et al., 2010). These have been reported as transient modules; but some indication of what might be comparable septa in the adult macaque can be detected in our PV material (Figure 6).

CONCLUSION

In summary, we have demonstrated the persistence of NADPHd+ neurons in the corpus callosum of adult macaque monkeys. Their persistence in the adult and their apparent association with blood vessels argues for a role other than in axon guidance. Other possibilities as to their function include a role in widespread network organization, possibly related to sleep cycles, or in interactions of axons, myelination, and vasculature. Multiple roles of NOS are summarized in Calabrese et al., 2007. Presumably, since a role in axon guidance has been repeatedly demonstrated for transient intracallosal neurons (Riederer et al., 2004; Niquille et al., 2009), these neurons undergo changing roles over the course of the lifetime (Friedlander and Torres-Reveron, 2009).

ACKNOWLEDGMENTS

We would like to thank Professors E. Vaucher and E. Hamel for kind discussion. Funding is gratefully acknowledged from RIKEN Brain Science Institute, and the RIKEN-MIT Center for Neural Circuit Genetics.

REFERENCES

- Calabrese, V., Mancuso, C., Calvani, M., Rizzarelli, E., Butterfield, D. A., and Stella, A. M. (2007). Nitric oxide in the central nervous system: neuroprotection versus neurotoxicity. *Nat. Rev. Neurosci.* 8, 766–775.
- Cauli, B., and Hamel, E. (2010). Revisiting the role of neurons in neurovascular coupling. *Front. Neuroenergetics* 2:9. doi:10.3389/fnene.2010.00009
- Cauli, B., Tong, X. K., Rancillac, A., Serluca, N., Lambolez, B., Rossier, J., and Hamel, E. (2004). Cortical GABA interneurons in neurovascular coupling: relays for subcortical vasoactive pathways. *J. Neurosci.* 24, 8940–8949.
- Chun, J. J., and Shatz, C. J. (1989). Interstitial cells of the adult neocortical white matter are the remnant of the early generated subplate neuron population. *J. Comp. Neurol.* 282, 555–569.
- Clancy, B., Silva-Filho, M., and Friedlander, M. J. (2001). Structure and projections of white matter neurons in the postnatal rat visual cortex. *J. Comp. Neurol.* 434, 233–252.
- Estrada, C., and DeFelipe, J. (1998). Nitric oxide-producing neurons in the neocortex: morphological and functional relationship with intraparenchymal microvasculature. *Cereb. Cortex* 8, 193–203.
- Friedlander, M. J., and Torres-Reveron, J. (2009). The changing roles of neurons in the cortical subplate. *Front. Neuroanat.* 3:15. doi:10.3389/neuro.05.015.2009
- García-Marín, V., Blazquez-Llorca, L., Rodríguez, J. R., Gonzalez-Soriano, J., and DeFelipe, J. (2010). Differential distribution of neurons in the gyral white matter of the human cerebral cortex. *J. Comp. Neurol.* 518, 4740–4759.
- Garthwaite, G., Bartus, K., Malcolm, D., Goodwin, D., Kollb-Sielecka, M., Dooleniya, C., and Garthwaite, J. (2006). Signaling from blood vessels to CNS axons through nitric oxide. *J. Neurosci.* 26, 7730–7740.
- Geneser-Jensen, F. A., and Blackstad, T. W. (1971). Distribution of acetyl cholinesterase in the hippocampal region of the guinea pig. I. Entorhinal area, parasubiculum, and pre-subiculum. *Z. Zellforsch. Mikrosk. Anat.* 114, 460–481.
- Hamel, E. (2006). Perivascular nerves and the regulation of cerebrovascular tone. *J. Appl. Physiol.* 100, 1059–1064.
- Higo, S., Akashi, K., Sakimura, K., and Tamamaki, N. (2009). Subtypes of GABAergic neurons project axons in the neocortex. *Front. Neuroanat.* 3:25. doi:10.3389/neuro.05.025.2009
- Iadecola, C. (2004). Neurovascular regulation in the normal brain and in Alzheimer's disease. *Nat. Rev. Neurosci.* 5, 347–360.
- Ichinohe, N., Watakabe, A., Miyashita, T., Yamamori, T., Hashikawa, T., and Rockland, K. S. (2004). A voltage-gated potassium channel, Kv3.1b, is expressed by a subpopulation of large pyramidal neurons in layer 5 of the macaque monkey cortex. *Neuroscience* 129, 179–185.
- Jovanov-Milošević, N., Culjat, M., and Kostovic, I. (2009). Growth of the human corpus callosum: modular and laminar morphogenetic zones. *Front. Neuroanat.* 3:6. doi:10.3389/neuro.05.006.2009
- Jovanov-Milošević, N., Petanjek, Z., Petrovic, D., Judaš, M., and Kostovic, I. (2010). Morphology, molecular phenotypes and distribution of neurons in developing human corpus callosum. *Eur. J. Neurosci.* 32, 1423–1432.
- Kalinchuk, A. V., McCarley, R. W., Porkka-Heiskanen, T., and Basheer, R. (2010). Sleep deprivation triggers inducible nitric oxide-dependent nitric oxide production in wake-active basal forebrain neurons. *J. Neurosci.* 30, 13254–13264.

- Kara, P., and Friedlander, M. J. (1998). Dynamic modulation of cerebral cortex synaptic function by nitric oxide. *Prog. Brain Res.* 118, 183–198.
- Kilduff, T. S., Cauli, B., and Gerashchenko, D. (2011). Activation of cortical interneurons during sleep: an anatomical link to homeostatic sleep regulation? *Trends Neurosci.* 34, 10–19.
- Kocharyan, A., Fernandes, P., Tong, X. K., Vaucher, E., and Hamel, E. (2008). Specific subtypes of cortical GABA interneurons contribute to the neurovascular coupling response to basal forebrain stimulation. *J. Cereb. Blood Flow Metab.* 28, 221–231.
- Kostovic, I., and Rakic, P. (1980). Cytology and time of origin of interstitial neurons in the white matter in infant and adult human and monkey telencephalon. *J. Neurocytol.* 9, 219–242.
- Kukley, M., Capetillo-Zarate, E., and Dietrich, D. (2007). Vesicular glutamate release from axons in white matter. *Nat. Neurosci.* 10, 311–320.
- Lecrux, C., and Hamel, E. (2011). The neurovascular unit in brain function and disease. *Acta Physiol.* 203, 47–59.
- Niquille, M., Gareil, S., Mann, F., Hornung, J. P., Otsmane, B., Chevalley, S., Parras, C., Guillemot, F., Gaspar, P., Yanagawa, Y., and Lebrand, C. (2009). Transient neuron populations are required to guide callosal axons: a role for semaphorin 3C. *PLoS Biol.* 7, e1000230. doi:10.1371/journal.pbio.1000230
- Riederer, B. M., Berbel, P., and Innocenti, G. M. (2004). Neurons in the corpus callosum of the cat during postnatal development. *Eur. J. Neurosci.* 19, 2039–2046.
- Sandell, J. H. (1986). NADPH diaphorase histochemistry in the macaque striate cortex. *J. Comp. Neurol.* 251, 388–397.
- Scherer-Singler, U., Vincent, S. R., Kimura, H., and McGeer, E. G. (1983). Demonstration of a unique population of neurons with NADPH-diaphorase histochemistry. *J. Neurosci. Methods* 9, 229–234.
- Stys, P. K. (2011). The axo-myelinic synapse. *Trends Neurosci.* 34, 393–400.
- Suarez-Sola, M. L., Gonzalez-Delgado, F. J., Pueyo-Morlans, M., Medina-Bolivar, O. C., Hernandez-Acosta, N. C., Gonzalez-Gomez, M., and Meyer, G. (2009). Neurons in the white matter of the adult human neocortex. *Front. Neuroanat.* 3:7. doi:10.3389/neuro.05.007.2009
- Tomioka, R., Okamoto, K., Furuta, T., Fujiyama, F., Iwasato, T., Yanagawa, Y., Obata, K., Kaneko, T., and Tamamaki, N. (2005). Demonstration of long-range GABAergic connections distributed throughout the mouse neocortex. *Eur. J. Neurosci.* 21, 1587–1600.
- Tomioka, R., and Rockland, K. S. (2007). Long-distance corticocortical GABAergic neurons in the adult monkey white and gray matter. *J. Comp. Neurol.* 505, 526–538.
- Vaucher, E., Linville, D., and Hamel, E. (1997). Cholinergic basal forebrain projections to nitric oxide synthase-containing neurons in the rat cerebral cortex. *Neuroscience* 79, 827–836.
- von Engelhardt, J., Khrulev, S., Eliava, M., Wahlster, S., and Monyer, H. (2011). 5-HT3A receptor-bearing white matter interstitial GABAergic interneurons are functionally integrated into cortical and subcortical networks. *J. Neurosci.* 31, 16844–16854.
- Wood, J., and Garthwaite, J. (1994). Models of the diffusional spread of nitric oxide: implications for neural nitric oxide signalling and its pharmacological properties. *Neuropharmacology* 33, 1235–1244.
- Yan, X. X., Jen, L. S., and Garey, L. J. (1996). NADPH-diaphorase positive neurons in primate cerebral cortex colocalize with GABA and calcium-binding proteins. *Cereb. Cortex* 6, 524–529.
- Zhong, Y. M., and Rockland, K. S. (2003). Inferior parietal lobule projections to anterior inferotemporal cortex (area TE) in macaque monkey. *Cereb. Cortex* 13, 527–540.

Conflict of Interest Statement: The authors declare that the research was conducted in the absence of any commercial or financial relationships that could be construed as a potential conflict of interest.

Received: 05 January 2012; paper pending published: 18 January 2012; accepted: 01 February 2012; published online: 20 February 2012.

Citation: Rockland KS and Nayyar N (2012) Association of type I neurons positive for NADPH-diaphorase with blood vessels in the adult monkey corpus callosum. *Front. Neural Circuits* 6:4. doi: 10.3389/fncir.2012.00004

Copyright © 2012 Rockland and Nayyar. This is an open-access article distributed under the terms of the Creative Commons Attribution Non Commercial License, which permits non-commercial use, distribution, and reproduction in other forums, provided the original authors and source are credited.